ELSEVIER

www.elsevier.nl/locate/jorganchem

Journal of Organometallic Chemistry 600 (2000) 84–93

Journal of Organometallic Chemistry

Precursors of quadruply bridging phosphorus monoxide ligands: synthesis and structural characterization of a new family of anionic fluoro and alkoxyphosphinidene clusters $Ru_5(CO)_{15}(\mu_4\text{-}PR)$ ($R = N^iPr_2$, NCy_2, F, OMe, OEt, O^iPr): generation and structure of $[H_2NCy_2][Ru_5(CO)_{15}(\mu_4\text{-}PO)]$

John H. Yamamoto [a], Ludmila Scoles [a], Konstantin A. Udachin [a], Gary D. Enright [a], Arthur J. Carty [a,b,*]

[a] *Steacie Institute for Molecular Sciences, National Research Council of Canada, 100 Sussex Drive, Ottawa, Ont., Canada K1A OR6*
[b] *Department of Chemistry, Ottawa-Carleton Chemistry Institute, University of Ottawa, Ottawa, Ont., Canada K1N 6N5*

Received 21 October 1999; received in revised form 14 January 2000

Abstract

A new family of phosphorus functionalized, pentanuclear ruthenium clusters $Ru_5(CO)_{15}(\mu_4\text{-}PR)$ [$R = N^iPr_2$, NCy_2, F, OMe, OEt, O^iPr, O^-] has been synthesized and representative compounds structurally characterized. The reaction of $Ru_4(CO)_{13}(\mu_3\text{-}PNR_2)$ (**1**) (R = Cy, ^{i}Pr) with $Ru_3(CO)_{12}$ in refluxing heptane yields $H_2Ru_3(CO)_9(\mu_3\text{-}PNR_2)$ (**2**) and $Ru_5(CO)_{15}(\mu_4\text{-}PNR_2)$ (**3**). An alternative high-yield synthesis for **3** is the reaction of **1** with $Ru(CO)_5$ in refluxing hexane. Treatment of **3** with $HBF_4{\cdot}Et_2O$ produces $Ru_5(CO)_{15}(\mu_4\text{-}PF)$ (**4**) in high yield. In contrast, refluxing **3** with $HBF_4{\cdot}H_2O$ in CH_2Cl_2 yields **4** and $[R_2NH_2][Ru_5(CO)_{15}(\mu_4\text{-}PO)]$ (**5**), a cluster containing a μ_4-phosphorus monoxide (PO) ligand. The reaction of **4** with alcohols affords the series of alkoxy phosphinidene cluster complexes $Ru_5(CO)_{15}(\mu_4\text{-}POR')$ (**6**) (R' = Me, Et, ^{i}Pr). The structures of **2a** ($R = NCy_2$), **3a** ($R = NCy_2$), **4** (R = F), and the phosphorus monoxide cluster $[H_2NCy_2][Ru_5(CO)_{15}(\mu_4\text{-}PO)]$ (**5a** and **6a**) (R' = Me) have been determined by X-ray diffraction studies.

Keywords: Phosphinidene; Fluorophosphinidene; Alkoxyphosphinidene clusters; Phosphorus monoxide

1. Introduction

Phosphorus monoxide (PO) and diphosphorus monoxide (P_2O) are the simplest binary oxides of phosphorus. They have both been characterized spectroscopically in matrices and in molecular beams [1], but they are not reagents in a bottle since they are unstable with respect to the normal oxides P_4O_6 and P_4O_{10}. In contrast to nitrogen monoxide, NO, which has been studied extensively as a ligand [2], complexes containing coordinated PO and P_2O have only been described very recently [3–7]. For phosphorus monoxide, two synthetic methodologies have emerged [3,4]: the direct oxidation of a coordinated naked phosphorus atom in a mono- [5] or polynuclear phosphide complex [3,6] and the hydrolytic cleavage of a P–N bond in an anionic phosphinidene cluster followed by deprotonation of the resulting hydroxyphosphinidene ligand [4].

The first transition-metal complex containing a PO ligand was synthesized by air oxidation of the naked phosphorus atoms in the diphosphorus cluster $[\eta^5\text{-}(C_5H^iPr_4)Ni(\mu_3\text{-}P)]_2W(CO)_4$ to form the complex $[\eta^5\text{-}(C_5H^iPr_4)Ni(\mu_3\text{-}PO)]_2W(CO)_4$ [3]. This molecule has two μ_3-PO ligands bridging open faces of a WNi_2 triangle. Subsequent to the seminal work of Scherer et al. [3], we reported for the first time the generation of clusters containing PO ligands via the hydrolysis of aminophosphinidene complexes [4]. This is a potentially powerful method of accessing coordinated PO ligands. The cleavage of P–NR_2 bonds can be accomplished via a multistep process that involves protonation with strong acid

* Corresponding author. Fax: +1-613-9578850.
E-mail address: arthur.carty@nrc.ca (A.J. Carty)

0022-328X/00/$ - see front matter
PII: S0022-328X(00)00033-4

($HBF_4 \cdot Et_2O$), sequential replacement of a NR_2 group by fluorine and of the fluoro ligand by an OH functionality to yield an hydroxyphosphinidene (μ_3-POH) ligand. Subsequent deprotonation of the μ_3-POH group by base affords a μ_3-PO^- ligand [4c]. Several μ_3-PO complexes have been prepared by this route [4]. An alternative, but less attractive, strategy is the simple hydrolysis of μ-PNR_2 ligands on acidic silica [4a,b]. Very recently, a mononuclear molybdenum phosphide has been oxidized to form the first example of a metal complex containing a η^1-PO ligand [5]. The direct oxidation of naked phosphides has been extended to other homo- and polynuclear clusters [6].

Until recently only the two coordination modes μ_3 and η^1 were known for the phosphorus monoxide ligand. Thus, we undertook the present work in an attempt to expand the range of phosphorus monoxide complexes accessible via the P–N cleavage route and to synthesize an example of a quadruply bridging μ_4-PO ligand specifically. There is as yet no known example of an analogous μ_4-NO ligand. The synthetic strategy adopted for the synthesis of the anionic μ_4-PO cluster $[Ru_5(CO)_{15}(\mu_4\text{-PO})]^-$ involved the generation of the pentanuclear cluster $Ru_5(CO)_{15}(\mu_4\text{-}PNR_2)$ from the tetranuclear $Ru_4(CO)_{13}(\mu_3\text{-}PNR_2)$ followed by treatment of the former with $HBF_4 \cdot H_2O$ to effect the hydrolytic P–N bond cleavage and formation of a P–O bond. However, we also observed that the reaction of $Ru_5(CO)_{15}(\mu_4\text{-}PNR_2)$ with anhydrous $HBF_4 \cdot Et_2O$ led to the isolation of a fluorophosphinidene cluster $Ru_5(CO)_{15}(\mu_4\text{-PF})$, which in turn could be used as a precursor of a series of alkoxy phosphinidene complexes $Ru_5(CO)_{15}(\mu_4\text{-POR})$. The synthesis of this family of phosphinidene complexes and the cluster **5** containing a μ_4-PO ligand are described herein. A preliminary account of part of this work has been published [7].

2. Experimental

Unless specified otherwise, all reactions were carried out under an atmosphere of nitrogen. All solvents were appropriately dried prior to use. The acids $HBF_4 \cdot Et_2O$ and $HBF_4 \cdot H_2O$ were purchased from Aldrich and used without further purification. Clusters $Ru_4(CO)_{13}(\mu_3\text{-}PNCy_2)$ (**1a**) [7] and $Ru_4(CO)_{13}(\mu_3\text{-}PN^iPr_2)$ (**1b**) [4a] as well as $Ru(CO)_5$ [8] were synthesized by known procedures. TLC separations were performed in air using homemade silica gel plates (60 Å F254) (CAMAG, 0.50 nm). Ms Ann Webb of the Institute of Biological Sciences at the National Research Council of Canada performed the elemental analyses. ^{19}F-NMR spectra were obtained with a Bruker AMX-500 spectrometer at 470.45 MHz. ^{19}F-NMR spectra were referenced to CF_3COOH, which was given a chemical shift of 0.00 ppm. ^{1}H- and ^{31}P-NMR spectra were obtained with a Bruker DRX-400 spectrometer. ^{31}P-NMR spectra were referenced to a sealed capillary of 80% phosphoric acid in a NMR tube containing $CDCl_3$. ^{31}P and ^{1}H spectra were collected at 162.02 and 400.13 MHz, respectively. IR spectra were recorded on a Bio-Rad FTS-40A FTIR spectrometer.

2.1. Synthesis of 2a and 3a

A sample of $Ru_4(CO)_{13}(\mu_3\text{-}PNCy_2)$ (**1a**) (327 mg, 0.33 mmol) was placed in a three-necked flask with 74 mg of $Ru_3(CO)_{12}$ (0.12 mmol) and 25 ml of dry heptane. The solution was refluxed for 1 h and then dried in vacuo. The green solid was chromatographed on a silica gel TLC plate in air with hexane as the eluting solvent. The compounds isolated in order of elution were: $H_2Ru_3(CO)_9(\mu_3\text{-}PNCy_2)$ (**2a**) (40 mg, 0.05 mmol, 15%) and $Ru_5(CO)_{15}(\mu_4\text{-}PNCy_2)$ (**3a**) (262 mg, 0.23 mmol, 70%). Spectral data for $H_2Ru_3(CO)_9(\mu_3\text{-}PNCy_2)$ (**2a**). IR, (ν(CO), in hexane), 2097 w, 2069 s, 2044 vs, 2037 m, 2016 s, 1993 w, 1978 w cm^{-1}. ^{1}H-NMR, (δ, $CDCl_3$), 3.15 (bs, 2H), 1.81 (m, 8H), 1.67 (m, 6H), 1.29 (m, 4H), 1.14 (m, 2H), −18.56 (d, 2H, $J_{P-H} = 14.5$ Hz). ^{31}P{^{1}H}-NMR, (δ, $CDCl_3$), 306.9 s. Anal. Calc. for $C_{21}H_{24}NO_9PRu_3$ (**2a**): C, 32.82; H, 3.15; N, 1.82. Found: C, 33.10; H, 3.54; N, 2.07%. Spectral data for $Ru_5(CO)_{15}(\mu_4\text{-}PNCy_2)$ (**3a**). IR, (ν(CO) in hexane), 2091 w, 2050 vs, 2031 m, 2000 w, 1989 w cm^{-1}. ^{1}H-NMR, (δ, $CDCl_3$), 3.52 (m, 2H), 1.78 (m, 8H), 1.62 (m, 8H), 1.24 (m, 2H). ^{31}P{^{1}H}-NMR, (δ, $CDCl_3$), 490 s. Anal. Calc. for $C_{27}H_{22}NO_{15}PRu_5$ **3a**: C, 28.53; H, 1.95; N, 1.23. Found: C, 28.05; H, 1.85; N, 1.19%.

2.2. Synthesis of 2b and 3b

A sample of $Ru_4(CO)_{13}(\mu_3\text{-}PN^iPr_2)$ (**1b**) (250 mg, 0.28 mmol) was placed in a three-necked flask with 300 mg of $Ru_3(CO)_{12}$ (0.46 mmol) and 25 ml of dry heptane. The solution was refluxed for 30 min and then dried in vacuo. The green solid was chromatographed on a silica gel TLC plate with hexane as the eluting solvent. The compounds isolated in order of elution were: $H_2Ru_3(CO)_9(\mu_3\text{-}PN^iPr_2)$ (**2b**) (40 mg, 0.06 mmol, 21%) and $Ru_5(CO)_{15}(\mu_4\text{-}PN^iPr_2)$ (**3b**) (240 mg, 0.22 mmol, 78%). Spectral data for $H_2Ru_3(CO)_9(\mu_3\text{-}PN^iPr_2)$ (**2b**). IR, (ν(CO) in hexane), 2098 w, 2070 s, 2045 vs, 2038 m, 2018 s, 1996 w, 1981 w cm^{-1}. ^{1}H-NMR, (δ, $CDCl_3$), 3.91 (dq, 12H, $J_{H-H} = 6.80$), 1.34 (d, 12H, $J_{H-H} = 6.80$), −18.62 (d, 2H, $J_{P-H} = 14.6$ Hz). ^{31}P{^{1}H}-NMR, (δ, $CDCl_3$), 330.3 s. Anal. Calc. for $C_{15}H_{16}NO_9PRu_3$ (**2b**): C, 26.16; H, 2.34; N, 2.03. Found: C, 26.38; H, 2.35; N, 1.95%. Spectral data for $Ru_5(CO)_{15}(\mu_4\text{-}PN^iPr_2)$ (**3b**). IR, (ν(CO) in hexane), 2090 w, 2050 vs, 2031 m, 2000 w, 1988 w cm^{-1}. ^{1}H-NMR, (δ, $CDCl_3$), 3.92 (q, 1H, $J_{H-H} = 7.00$ Hz), 3.87 (q, 1H, $J_{H-H} = 7.00$ Hz), 1.25 (d, 12h, $J_{H-H} = 7.00$ Hz). ^{31}P-NMR, (δ, $CDCl_3$), 489.3 s.

Anal. Calc. for $C_{21}H_{14}NO_{15}PRu_5$ (**3b**): C, 23.87; H, 1.34; N, 1.33. Found: C, 24.32; H, 1.40; N, 1.23%.

2.3. Synthesis of *3a*

A sample of $Ru_4(CO)_{13}(\mu_3\text{-}PNCy_2)$ (**1a**) (770 mg, 0.78 mmol) was placed in a three-necked flask with 1000 ml of a hexane solution of $Ru(CO)_5$ (0.75 mg ml^{-1}). The solution was refluxed for 8 h and then dried in vacuo. The green solid was chromatographed on a silica gel column (2 × 10 cm) in air with hexane as the eluting solvent. The compounds isolated in order of elution were: $Ru_3(CO)_{12}$ (5 mg, 0.008 mmol, 1%); $Ru_5(CO)_{15}(\mu_4\text{-}PNCy_2)$ (**3a**) (867 mg, 0.76 mmol, 97%).

2.4. Synthesis of *3b*

A sample of $Ru_4(CO)_{13}(\mu_3\text{-}PN^iPr_2)$ (**1b**) (381 mg, 0.39 mmol) was placed in a three-necked flask with 400 ml of a hexane solution of $Ru(CO)_5$ (1 mg ml^{-1}). The solution was refluxed for 8 h and then dried in vacuo. The green solid was chromatographed on a silica gel column in air with hexane as the eluting solvent. The two compounds isolated in order of elution were: $Ru_3(CO)_{12}$ (10 mg, 0.015 mmol, 4%); $Ru_5(CO)_{15}(\mu_4\text{-}PN^iPr_2)$ (**3b**) (412 mg, 0.39 mmol, 92%).

2.5. Synthesis of *4* from *3a* and *3b*

The cluster $Ru_5(CO)_{15}(\mu_4\text{-}PNCy_2)$ (**3a**) (503 mg, 0.51 mmol) was placed in a 100 ml round-bottom flask with 50 ml of dry CH_2Cl_2 and 300 μl of $HBF_4{\cdot}Et_2O$ was added to the green solution. The solution was allowed to stir for 24 h at room temperature (r.t.), and then was dried in vacuo. The green solid was placed on top of a silica gel column and a single compound was eluted with hexane. This green compound was determined to be $Ru_5(CO)_{15}(\mu_4\text{-}PF)$ (**4**) (481 mg, 0.49 mmol, 96%). Spectral data for $Ru_5(CO)_{15}(\mu_4\text{-}PF)$ (**4**). IR, (ν(CO), hexane), 2068 vs, 2039 s, 2024 w, 2004 w cm^{-1}. ^{31}P-NMR, (δ, $CDCl_3$), 548.6 d ($J_{P-F} = 1121$ Hz). ^{19}F-NMR, (δ, $CDCl_3$ vs. CF_3COOH), −20.49 d ($J_{P-F} = 1121$ Hz). Anal. Calc. for $C_{15}O_{15}FPRu_5$ (**4**): C, 18.47; H, 0.00. Found: C, 18.50; H, 0.00%.

A similar reaction between $Ru_5(CO)_{15}(\mu_4\text{-}PN^iPr_2)$ (**3b**) (375 mg, 0.42 mmol) in CH_2Cl_2 (10 ml) with $HBF_4{\cdot}Et_2O$ (200 μl) afforded cluster **4** (350 mg, 0.36 mmol) in 85% yield.

2.6. Synthesis of *5a*

The cluster $Ru_5(CO)_{15}(\mu_4\text{-}PNCy_2)$ (**3a**) (57 mg, 0.05 mmol) was placed in a 25 ml flask with 20 ml of dry CH_2Cl_2 and 200 μl of $HBF_4{\cdot}H_2O$. The solution was refluxed for 19 h, and then was dried in vacuo. The green solid was placed on top of a silica gel TLC plate and the single green compound eluted with hexane was found to be $Ru_5(CO)_{15}(\mu_4\text{-}PF)$ (**4**) (15 mg, 0.015 mmol, 31%). The green base line was eluted with acetone to yield a green salt $[H_2NCy_2][Ru_5(CO)_{15}(\mu_4\text{-}PO)]$ (**5a**) (37 mg, 0.032 mmol, 64%). Spectral data for $[H_2NCy_2][Ru_5(CO)_{15}(\mu_4\text{-}PO)]$ (**5a**). IR, (ν(CO), CH_2Cl_2), 2061 m, 2044 vs, 2031 m, 2013 s cm^{-1}. IR, (ν, (PO) CH_2Cl_2), 1064 w cm^{-1}. ^1H-NMR, (δ, $CDCl_3$), 6.72 (bs, 2H), 3.06 (m, 2H), 2.00 (d, 4H, $J_{H-H} = 11.30$ Hz), 1.90 (d, 4H, $J_{H-H} = 11.61$ Hz), 1.70 (d, 2H, $J_{H-H} = 10.63$ Hz), 1.45–1.18 (m, 10H). $^{31}P\{^1H\}$-NMR, (δ, $CDCl_3$), 515 s. Anal. Calc. for $C_{27}H_{24}NO_{16}PRu_5$ (**5a**): C, 28.08; H, 2.09; N, 1.21. Found: C, 28.02; H, 2.11; N, 1.1%.

2.7. Synthesis of *5b*

The cluster $Ru_5(CO)_{15}(\mu_4\text{-}PN^iPr_2)$ (**2b**) (500 mg, 0.44 mmol) was placed in a 50 ml flask with 25 ml of dry CH_2Cl_2 and 2000 μl of $HBF_4{\cdot}H_2O$. The solution was refluxed for 19 h, and then was dried in vacuo. The green solid was placed on top of a silica gel TLC plate and a single green compound eluted with hexane was determined to be $Ru_5(CO)_{15}(\mu_4\text{-}PF)$ (**4**) (110 mg, 0.10 mmol, 23%). The green base line was eluted with acetone to yield a green salt of $[H_2N^iPr_2][Ru_5(CO)_{15}(\mu_4\text{-}PO)]$ (**5b**) (260 mg, 0.27 mmol, 60%). Spectral data for $[H_2N^iPr_2][Ru_5(CO)_{15}(\mu_4\text{-}PO)]$ (**5b**). IR, (ν(CO), CH_2Cl_2), 2061 s, 2045 vs, 2031 m, 2014 s cm^{-1}. IR, (ν, (PO) CH_2Cl_2), 1063 w cm^{-1}. ^1H-NMR, (δ, $CDCl_3$), 3.34 (m, 2H), 1.32 (d, 6H, $J_{H-H} = 6.5$ Hz). $^{31}P\{^1H\}$-NMR, (δ, $CDCl_3$), 514 s. Anal. Calc. for $C_{21}H_{16}NO_{16}PRu_5$ (**5b**): C, 23.46; H, 1.50; N, 1.30. Found: C, 23.66; H, 2.41; N, 1.36%.

2.8. Synthesis of *6a*

The cluster $Ru_5(CO)_{15}(\mu_4\text{-}PF)$ (**4**) (67 mg, 0.07 mmol) was placed in a 25 ml Schlenk tube with 10 ml of MeOH. This solution was heated to reflux for 24 h. The solution was dried in vacuo and the green residue was separated on a silica gel TLC plate with hexane as the eluting solvent. A single green band was isolated (68 mg, 0.70 mmol, 98%). Spectral data for $Ru_5(CO)_{15}(\mu_4\text{-}POMe)$ (**6a**). IR, (ν(CO), hexane), 2098 vw, 2061 vs, 2033 s, 1999 w cm^{-1}. ^1H-NMR, (δ, $CDCl_3$), 3.45 (d, 3H, $J_{P-H} = 16.68$ Hz). $^{31}P\{^1H\}$-NMR, (δ, $CDCl_3$), 542.8 s. Anal. Calc. for $C_{16}H_3O_{16}PRu_5$ (**6a**): C, 19.46; H, 0.31. Found: C, 20.25; H, 0.38%.

2.9. Synthesis of *6b*

The cluster $Ru_5(CO)_{15}(\mu_4\text{-}PF)$ (**4**) (31 mg, 0.03 mmol) was placed in a 25 ml Schlenk tube with 20 ml of

EtOH. This solution was heated to reflux for 24 h. The solution was dried in vacuo and the green residue was separated on a silica gel TLC plate with hexane as the eluting solvent. A single green band was isolated (20 mg, 0.02 mmol, 67%). Spectral data for $Ru_5(CO)_{15}(\mu_4$-POEt) (**6b**). IR (ν(CO), hexane), 2097 vw, 2060 vs, 2033 m, 1998 w cm^{-1}. ^{1}H-NMR, (δ, $CDCl_3$), 3.59 (m, 2H), 1.22 (t, 3H, $J_{H-H} = 7.0$ Hz). $^{31}P\{^1H\}$-NMR, (δ, $CDCl_3$), 537 s. Anal. Calc. for $C_{17}H_5O_{16}PRu_5$ (**6b**): C, 20.39; H, 0.50. Found: C, 20.06; H, 0.34%.

2.10. Synthesis of 6c

The cluster $Ru_5(CO)_{15}(\mu_4$-PF) (**4**) (51 mg, 0.052 mmol) was placed in a 25 ml Schlenk tube with 20 ml of ^{i}PrOH. This solution was heated to reflux for 7 h. The solution was dried in vacuo and the green residue was separated on a silica gel TLC plate with hexane as the eluting solvent. A single green band was isolated (11 mg, 0.01 mmol, 21%). Spectral data for $Ru_5(CO)_{15}(\mu_4$-PO^{i}Pr) (**6c**). IR, (ν(CO), hexane), 2081 vw, 2059 vs, 2032 s, 1997 w cm^{-1}. ^{1}H-NMR, (δ, $CDCl_3$), 3.91 (1H, m), 1.18 (6H, d, $J_{H-H} = 6.2$ Hz). $^{31}P\{^1H\}$-NMR, (δ, $CDCl_3$), 534 s. Anal. Calc. for $C_{18}H_7O_{16}PRu_5$ (**6c**): C, 21.29; H, 0.69. Found: C, 21.4; H, 0.93%.

3. Crystallographic analyses

Crystals of **2a**, **3a**, **4**, **5a** and **6a** suitable for X-ray diffraction analysis were grown by slow evaporation of a 1:2 CH_2Cl_2–hexane solution at −20°C. The crystals used in the diffraction measurements were mounted on a glass fiber with a 5 min epoxy. Diffraction measurements were made on a Siemens SMART CCD automatic diffractometer by using graphite-monochromated Mo–K_α radiation. The unit cells were determined from randomly selected reflections obtained by using the SMART CCD automatic search, center, index and least-squares routines. Crystal data, data collection parameters, and results of the analyses are listed in Table 1. Data processing for **2a**, **3a**, **4**, **6a** was performed on a Silicon Graphics INDY computer by using the NRCVAX [9] structure solving library obtained from the National Research Council of Canada, Ottawa, Ontario. Data processing for **5a** was done on a Pentium II computer using SHELXTL. Neutral atom scattering factors were taken from the standard references [10,11]. Anomalous dispersion corrections were applied to all non-hydrogen atoms [11]. Lorentz/polarization (Lp) and absorption corrections were applied to the data for all of the structures. Full-matrix least-square refine-

Table 1
Crystallographic data for compounds **2a**, **3a**, **4**, **5a** and **6a**

	2a	**3a**	**4**	**5a**	**6a**
Formula	$Ru_3PNO_9C_{21}H_{24}$	$Ru_5PNO_{15}C_{27}H_{22}$	$Ru_5PO_{15}C_{15}F$	$Ru_5PO_{16}NCl_{0.5}C_{27.25}H_{24.5}$	$Ru_5PO_{16}C_{16}H_3$
Formula weight	768.60	1136.78	975.47	1176.02	987.50
Crystal system	Monoclinic	Monoclinic	Monoclinic	Triclinic	Monoclinic
Lattice parameters					
a (Å)	9.7179(4)	9.841(4)	9.6072(4)	10.241(2)	9.8734(4)
b (Å)	14.5862(7)	11.7210(5)	16.7952(7)	12.914(3)	16.0861(7)
c (Å)	19.5598(9)	29.7585(13)	15.4589(7)	30.897(6)	15.8976(7)
α (°)	90	90	90	91.52(3)	90
β (°)	92.82(1)	95.68(1)	100.65(1)	99.07(3)	95.49(1)
γ (°)	90	90	90	108.18(3)	90
V (Å^3)	2769.2(2)	3415.5(1)	2451.4(2)	3821.4(1)	2513.3(2)
Crystal dimensions (mm^3)	0.08 × 0.25 × 0.25	0.07 × 0.15 × 0.08	0.27 × 0.22 × 0.09	0.04 × 0.02 × 0.15	0.15 × 0.15 × 0.045
Space group	$P21/n$ (no. 14)	$P21/n$ (no. 14)	$P21/n$ (no. 14)	$P\bar{1}$ (no. 2)	$P21/n$ (no. 14)
Z	4	4	4	4	4
$\rho_{calc.}$ (Mg m^{-3})	1.84	2.21	2.64	2.08	2.61
μ(Mo–K_α) (mm^{-1})	1.72	2.28	3.15	2.04	3.08
T (°C)	−100	−100	−100	−100	−100
$2\theta_{max}$ (°)	57.5	57.5	57.5	50.0	57.5
Reflections measured	31137	38641	28166	26487	28396
Unique reflections	7138	8849	6349	13417	6511
Observations [$I > 2.5\sigma(I)$]	6612	6987	5396	9190	5693
Variables	412	531	334	1360	356
Goodness-of-fit	2.73	1.66	2.18	1.08	1.84
Max shift in final cycle	0.00	0.00	0.00	0.00	0.00
Residuals: R; R_w	0.025; 0.032	0.032; 0.027	0.033; 0.031	0.051; 0.090	0.025;0.025
Absorption correction	Empirical	Empirical	Empirical	Empirical	Empirical
Largest peak in final difference map (e Å^{-3})	0.58	1.05	0.97	1.04	1.05

ments minimized the function $\Sigma_{hkl} w(|F_o| - |F_c|)^2$ where $w = 1/\sigma(F_o)2$, $\sigma(F_o) = \sigma(F_o^2)/2F_o$ and $\sigma(F_o^2) = [\sigma(I_{raw})^2 + (0.02I_{net})^2]^{1/2}/Lp$.

The crystallographic space group $P2_1/n$ was uniquely identified for compounds **2a**, **3a**, **4** and **6a** by the pattern of systematic absences observed during the collection of intensity data. For compound **5a** the space group $P\bar{1}$ was assumed and was confirmed by successful solution and refinement of the structure. All structures were solved by a combination of direct methods and difference Fourier syntheses. All non-hydrogen atoms were refined with anisotropic thermal parameters.

4. Result and discussion

Although the coordination and organometallic chemistry of the binary nitrogen oxide NO has been studied extensively over many years, the same cannot be said of its heavier congener phosphorus monoxide PO. Indeed complexes of PO have only been described recently and at the outset of this work only μ_3- and η^1-coordination modes were known. A major factor inhibiting the development of PO as a ligand is the lack of synthetic methods for synthesizing PO complexes. Unlike NO, PO is not readily available as the free ligand since P_4O_6 and P_4O_{10}, which are cage compounds, are the normal oxides of phosphorus under ambient conditions. Thus access to PO complexes depends on the availability of indirect methods of synthesis from other precursors ligands. One route which has been used is that first described by Scherer et al. in the synthesis of $[\eta^5$-$(C_5H^iPr_4)Ni(\mu_3$-$P)]_2W(CO)_4$ [3], namely the direct oxidation of a preformed, naked phosphide ligand by air or a chemical oxidizing agent. Other workers [5,6] have used similar methodology to prepare μ_3-PO clusters and the first η^1-PO complex $Mo\{N[C(CD_3)_2Me][C_6H_3Me_2$-$3,5]\}_3(\eta^1$-P=O) was prepared by oxidation of a terminal η^1-P ligand with dimethyloxirane [5]. One of the shortcomings of this direct oxidation route, however, is the difficulty of accessing the appropriate precursor phosphide molecule.

Recently we have described a convenient and potentially versatile route to PO complexes, which formally involves the acid-catalyzed hydrolytic cleavage of the P–N bond of a coordinated aminophosphinidene ligand [4,7]. While overall the reaction involves the substitution of an NR_2 group of the μ-PNR_2 ligand by OH, followed by the deprotonation of the resulting hydroxyphosphinidene ligand μ-POH by the liberated base (HNR_2), we have shown that under anhydrous condition in the presence of $HBF_4 \cdot Et_2O$ substitution of an NR_2 group of a μ-PNR_2 ligand by fluorine occurs, affording previously unknown and stable but reactive fluorophosphinidene clusters. These latter μ-PF clusters can, in turn, be used as precursors of other phosphinidenes, including hydroxyphosphinidenes and their Bronsted bases, the anionic PO complexes. By adapting this general methodology we have expanded the range of coordination modes of phosphorus monoxide to include μ_4-PO bonding and prepared a family of new functionalized phosphinidene clusters.

Refluxing the versatile starting material $Ru_4(CO)_{13}(\mu_3$-$PNR_2)$ (**1a**, R = Cy; **1b**, R = ^{i}Pr) in the presence of an excess of $Ru_3(CO)_{12}$ forms two new cluster complexes, $H_2Ru_3(CO)_9(\mu_3$-$PNR_2)$ (**2a**, R = Cy; **2b**, R = ^{i}Pr) and $Ru_5(CO)_{15}(\mu_4$-$PNR_2)$ (**3a**, R = Cy; **3b**, R = ^{i}Pr) in 15–21% and 70–78% yields, respectively. A higher yield of $Ru_5(CO)_{15}(\mu_4$-$PNR_2)$ (**3**) (> 95%) can be obtained from the addition reaction of $Ru_4(CO)_{13}(\mu_3$-$PNR_2)$ (**1**) with $Ru(CO)_5$ in hexane for 8 h (Scheme 1). This synthesis is the first high-yield systematic synthesis of an $Ru_5(CO)_{15}(\mu_4$-phosphinidene) cluster complex. This methodology could be used to form other phosphinidenes with mixed metal cores M_4M' and different substituents on the PR group. Previously, $Ru_5(CO)_{15}$-$(\mu_4$-PR) (R = Ph, Me, Et, CH_2Ph) have been formed by the thermolysis of $[(\eta^5$-$C_5H_5)(CO)_2MnPRCl_2]$ with $Ru_3(CO)_{12}$ at 100°C for 48 h [12], or as minor products from the preparation of $Ru_4(CO)_{13}(\mu_3$-PPh) [13a], and $Ru_8(CO)_{21}(\mu_6$-P)$(\mu_4$-PPh)$(\mu_2$-$PPh_2)$ [13b]. These μ_4-phosphinidene complexes were formed in only 2.5–8% yields. The side products **2a** and **2b** are formed presumably via cluster fragmentation reactions and the capture of dihydrogen from the decomposition of PNR_2 ligands or alternatively from traces of water on the walls of the reaction vessel. Clusters **2a** and **2b** exhibit a doublet hydride resonance at high field (δ = −18.6) typical of hydrides bridging Ru–Ru bonds in clusters [13c]. A single-crystal X-ray analysis of **2a** confirmed the overall structure and the presence of edge bridging hydride ligands.

The reaction of $Ru_5(CO)_{15}(\mu_4$-$PNR_2)$ (**3a**, **b**) with anhydrous $HBF_4 \cdot Et_2O$ forms $Ru_5(CO)_{15}(\mu_4$-PF) (**4**) exclusively, in greater than 85% yield (Scheme 1). This type of reactivity, notably the formation of a fluorophosphinidene ligand by the acidic cleavage of an aminophosphinidene ligand with $HBF_4 \cdot OEt_2$, has been observed previously in the $M_4(CO)_{13}(\mu_3$-$PN^iPr_2)$ (M = Ru or Os) systems [4c].

A substantial difference in reactivity is observed for the reaction of $Ru_5(CO)_{15}(\mu_4$-PF) (**4**) and $Ru_4(CO)_{13}(\mu_3$-PF) with nucleophiles. The μ_4-fluorophosphinidene ligand appears to be less reactive to nucleophilic attack than the μ_3-fluorophosphinidene ligand. This difference in reactivity is illustrated by the reaction of MeOH with the two fluorophosphinidene complexes. Previous work has shown that $Ru_4(CO)_{13}(\mu_3$-PF) will react with MeOH in CH_2Cl_2 solution at r.t. to form $Ru_4(CO)_{13}$-$(\mu_3$-POMe) [4c]. In contrast, the reaction with $Ru_5(CO)_{15}(\mu_4$-PF) (**4**) occurs only when pure MeOH is

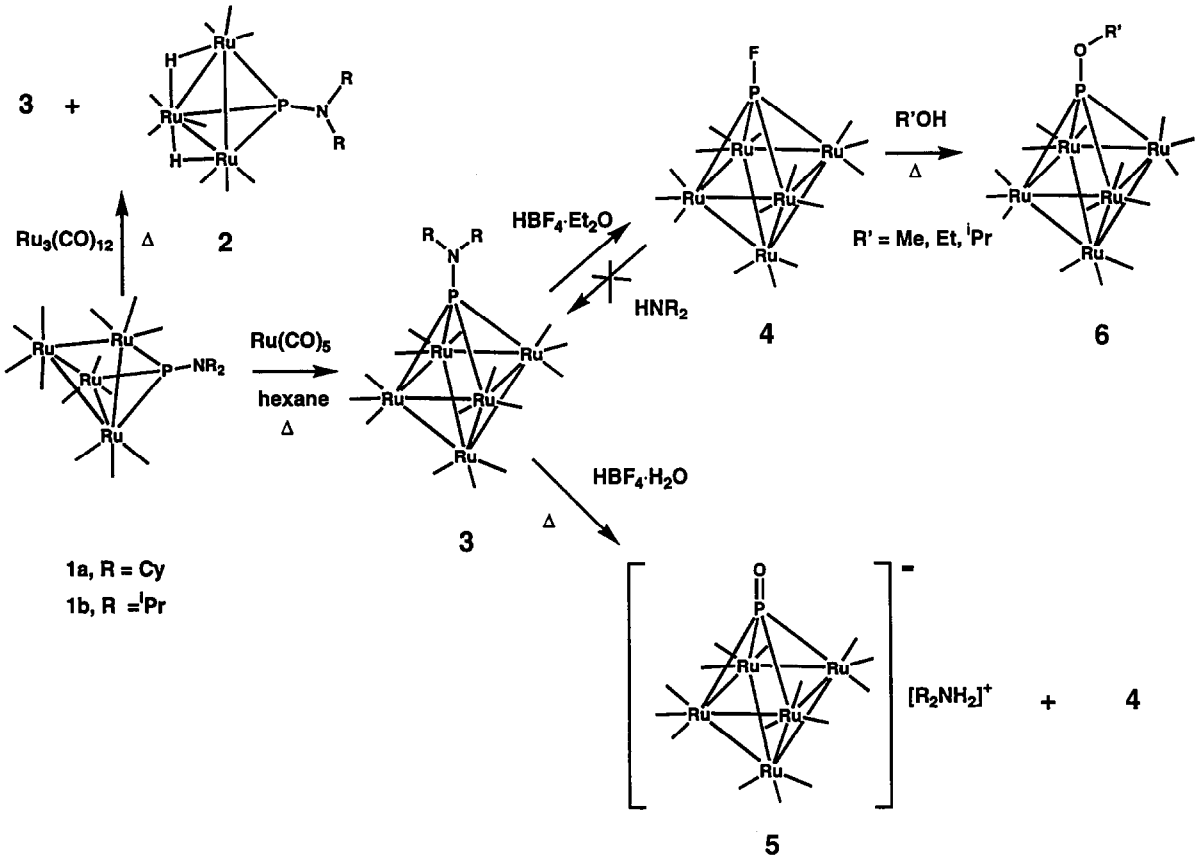

Scheme 1.

refluxed with the complexes for 24 h. Other alcohols such as EtOH, ^{i}PrOH, ^{t}BuOH were also used as reaction solvents for this reaction but there was a marked decrease in the yield of the desired product $Ru_5(CO)_{15}(\mu_4\text{-POR})$ (**6a–c**) with increasing bulkiness of the R-group of the alcohol. With ^{t}BuOH, no product was isolated. The analogous osmium complex to $Ru_5(CO)_{15}(\mu_4\text{-POMe})$ has been formed previously from the thermolysis of $Os_3(CO)_{11}P(OMe)_3$ [14].

The reactivities of $Ru_4(CO)_{13}(\mu_3\text{-PF})$ and $Ru_5(CO)_{15}(\mu_4\text{-PF})$ (**4**) towards other nucleophiles, such as H_2O, HNR_2 and MeLi, also differ. Thus $Ru_4(CO)_{13}(\mu_3\text{-PF})$ reacts to form the analogous μ_3-PR P–R complexes (R = OH, NR_2, Me) at r.t. but $Ru_5(CO)_{15}(\mu_4\text{-PF})$ fails to yield the analogous μ_4-PR complexes under the same reaction conditions.

The failure to transform the μ_4-PF ligand into a μ_4-POH group precluded the use of this precursor for the synthesis of the μ_4-PO ligand. However, a more direct route to the μ_4-PO ligand proved successful. The reaction of a CH_2Cl_2 solution of $Ru_5(CO)_{15}(\mu_4\text{-PNR}_2)$ (**3a, b**) with HBF_4 in water for 8 h formed the desired product $[R_2NH_2][Ru_5(CO)_{15}(\mu_4\text{-PO})]$ (**6**) in approximately 65% yield with $Ru_5(CO)_{15}(\mu_4\text{-PF})$ (**4**) being the only other complex isolated from this reaction. No substantial difference in yields was observed when different aminophosphinidene ligands, $PN^{i}Pr_2$ or $PNCy_2$ were used.

4.1. Structural determinations

The core features of the molecular structure of **2a**, shown in Fig. 1, consist of a dicyclohexyaminophosphinidene ligand triply bridging a triangle of three ruthenium atoms. The phosphinidene ligand is bonded to the triangular face of the three ruthenium atoms via two normal bond lengths (Ru(1)–P = 2.2833(6), Ru(3)–P = 2.2796(6) Å), and one long bond (2.3449(7) Å) to the unique Ru(2) atom, which is also bound to both hydride ligands. Each ruthenium atom has three terminal CO ligands arranged in a tripodal geometry. The P–N bond length of the aminophosphinidene ligand is 1.653(2) Å, which is intermediate between a P–N single bond (e.g. 1.769(2) Å for $NaPO_3NH_3$) [15] and a P=N double bond (e.g. 1.567(6) Å for $Ph_3P{=}NC_6H_4$-Br) [16]. The sum of the appropriate covalent radii of phosphorus and nitrogen give distances of 1.78 and 1.64 Å for PN single and double bonds, respectively [17]. This indicates that there is some PN double bond character in the aminophosphinidene ligand. The cyclohexyl groups of the aminophosphinidene ligands adopt the lowest-energy chair configuration. Two peaks were

identified by their location in the electron destiny map as being symmetrically bridging hydrides (Ru(1)–H(1) = 1.75(3), Ru(2)–H(1) = 1.84(3), Ru(2)–H(2) = 1.76(3), Ru(3)–H(2) = 1.81(3) Å). The peaks were refined both positionally and isotropically. Complexes with this structure, but differing in the R group, have been observed previously [18]. Assuming that the phosphinidene ligand is a four-electron donor, the molecule contains a total of 48 valence electrons and with three metal–metal bonds, is electron precise.

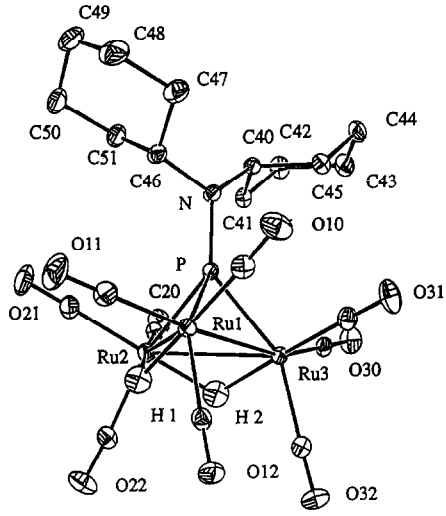

Fig. 1. An ORTEP diagram of $H_2Ru_3(CO)_9(\mu_3\text{-}PNCy_2)$ (**2a**) showing 30% probability thermal ellipsoids. Non-bridging hydrogen atoms or ligands were omitted for clarity. Selected bond lengths (Å) and angles (°): Ru(1)–Ru(2) = 2.9379(3), Ru(1)–Ru(3) = 2.8263(3), Ru(2)–Ru(3) = 2.9664(3), P–N = 1.653(2), Ru(2)–P = 2.3449(7), Ru(1)–P = 2.2833(6), Ru(3)–P = 2.2796(6), C(40)–N–C(46) = 117.41(19).

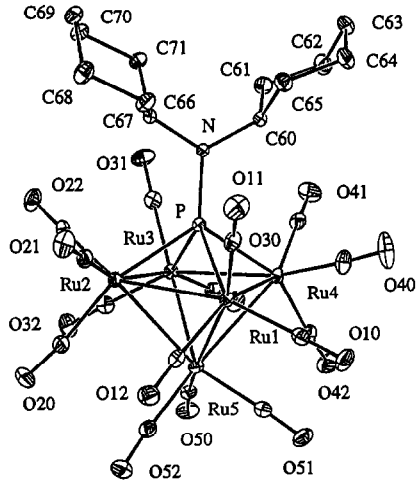

Fig. 2. An ORTEP diagram of $Ru_5(CO)_{15}(\mu_4\text{–}PNCy_2)$ (**3a**) showing 30% probability thermal ellipsoids. Hydrogen atoms were omitted for clarity. Selected bond lengths (Å) and angles (°): Ru(1)–Ru(2) = 2.9006(9), Ru(1)–Ru(4) = 2.9091(5), Ru(2)–Ru(3) = 2.8267(5), Ru(3)–Ru(4) = 2.8246(9), Ru(5)–Ru(3) = 2.8241(4), Ru(1)–Ru(5) = 2.7565(4), Ru(4)–Ru(5) = 2.8727(7), Ru(5)–Ru(2) = 2.8984(7), P–N = 1.681(3), Ru(1)–P = 2.455(1), Ru(3)–P = 2.482(1), Ru(2)–P = 2.347(1), Ru(4)–P = 2.368(1), C(60)–N–C(66) = 121.9(3).

The molecular structure of **3a** is shown in Fig. 2. Complex **3a** contains five ruthenium atoms arranged in a square-based pyramidal geometry. The square face of the cluster is capped with a μ_4-phosphinidene ligand. The phosphorus atom of the phosphinidene ligand is asymmetrically attached to the metal framework via two long Ru–P bonds Ru(1)–P = 2.455(1), Ru(3)–P = 2.482(1) Å and two shorter bond lengths Ru(4)–P = 2.368(1), Ru(2)–P = 2.347(1) Å. The short Ru–P distances lie almost in the PNR_2 plane, while the long distances are perpendicular to this plane, which may indicate that the two π-type frontier orbitals of the planar PNR_2 ligand are non-degenerate, have different energies and different bonding abilities with the two sets of ruthenium atoms. A similar but much more extreme distortion is found in the bis(phosphinidene) complexes $Ru_4(CO)_{12}(\mu_4\text{-}PNR_2)_2$ (R = ^{i}Pr, Et) [19] and has been the subject of a theoretical analysis [20]. Note that in $Ru_5(CO)_{15}PF$ and $[Ru_5(CO)_{15}PO]^-$ (vide infra) where π bonding can occur in both planes, the phosphorus ligands are bound more symmetrically. Ru–P distances in **3a** are all longer than in **2a**, since the P in **3a** is bound to the tetragonal face rather than a trigonal face as in **2a**. The four basal Ru–Ru bond lengths are in the range (2.8246–2.9091 Å). Each ruthenium atom has three terminal CO ligands. The P–N bond length of the aminophosphinidene ligand (1.681(3) Å) is again intermediate between a P–N single and double bond. Thus the PN bond in complex **3a** has some double-bond character. This is consistent with observations on other cluster complexes containing aminophosphinidene ligands (e.g. P–N for: $Ru_4(CO)_{13}(\mu_3\text{-}PN^iPr_2)$ = 1.671 Å [4b], $Ru_4(CO)_{11}(\mu_4\text{-}PN^iPr_2)(\mu_4\text{-}PPh)$ = 1.668(7) Å [19], $Os_4(CO)_{13}(\mu_3\text{-}PN^iPr_2)$ = 1.685(5) Å [4b] and $Ru_4(CO)_{12}(\mu_4\text{-}PNEt_2)_2$ = average 1.660 Å [20]). Complex **3a** with a total of 74 cluster valence electrons and eight metal–metal bonds in a square pyramidal metal array is electron precise. For the entire Ru_5P framework, there are seven skeletal electron pairs, appropriate for a six vertex *closo* structure.

Complex **4** (Fig. 3) consists of an octahedron of five ruthenium atoms each bearing three CO groups, together with the phosphorus atom of a μ_4-PF ligand. The fluorophosphinidene ligand is symmetrically bonded to four ruthenium atoms (Ru(1)–P = 2.3246(9); Ru(2)–P = 2.3024(10); Ru(3)–P = 2.3134(10) and Ru(4)–P = 2.2900(10) Å). The PF distance of 1.595(2) Å compares well with a value of 1.579 Å [21] for the P–F bonds in the hexafluorophosphate anion PF_6^-. Within the Ru_5 square pyramid there are two distinctively different sets of Ru–Ru distances with the bond lengths forming the square base (Ru–Ru average 2.920 Å) being significantly longer than those to the apical atom Ru(5) (Ru–Ru average 2.825 Å). The ^{19}F- and ^{31}P-NMR spectra of **4** both consist of doublets (δ^{19}F =

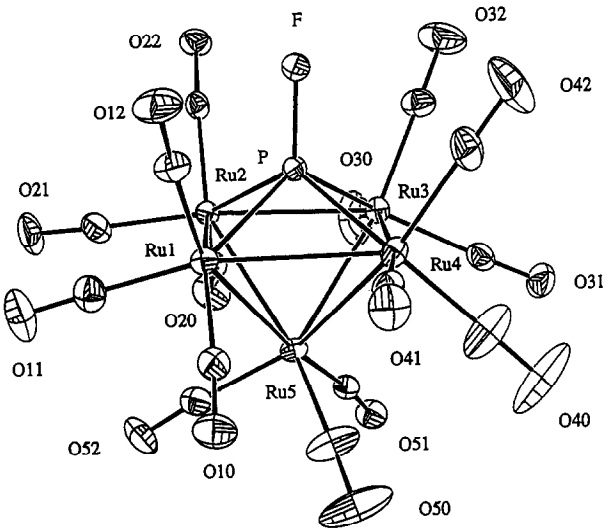

Fig. 3. An ORTEP diagram of $Ru_5(CO)_{15}(\mu_4\text{-PF})$ (**4**) showing 30% probability thermal ellipsoids. Hydrogen atoms were omitted for clarity. Selected bond lengths (Å) and angles (°): Ru(1)–Ru(2) = 2.9558(4), Ru(1)–Ru(4) = 2.9310(4), Ru(2)–Ru(3) = 2.8983(4), Ru(3)–Ru(4) = 2.8932(4), Ru(5)–Ru(3) = 2.8535(4), Ru(1)–Ru(5) = 2.7771(4), Ru(4)–Ru(5) = 2.8432(4), Ru(5)–Ru(2) = 2.8271(4), Ru(1)–P = 2.3246(9), Ru(2)–P = 2.3024(10), Ru(3)–P = 2.3134(10), Ru(4)–P = 2.2900(10), P–F = 1.595(2).

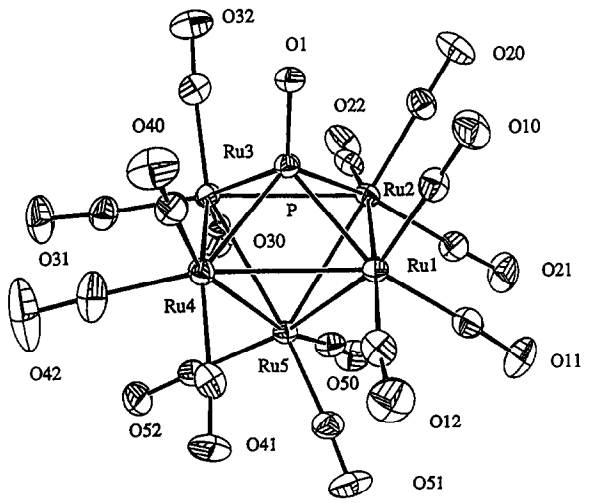

Fig. 4. An ORTEP diagram of the ordered molecule of $[H_2NCy_2][Ru_5(CO)_{15}(\mu_4\text{-PO})]$ (**5a**) showing 30% probability thermal ellipsoids. Hydrogen atoms and the cation $[H_2N(Cy)_2]^+$ were omitted for clarity. Selected bond lengths (Å) and angles (°): Ru(1)–Ru(2) = 2.851(1), Ru(1)–Ru(4) = 2.876(1), Ru(2)–Ru(3) = 2.893(1), Ru(3)–Ru(4) = 2.907(1), Ru(5)–Ru(3) = 2.798(1), Ru(1)–Ru(5) = 2.837(1), Ru(4)–Ru(5) = 2.803(1), Ru(5)–Ru(2) = 2.843(1), Ru(1)–P = 2.372(2), Ru(2)–P = 2.382(2), Ru(3)–P = 2.369(2), Ru(4)–P = 2.372(2), P–O = 1.512(5).

−20.49; ^{31}P 548.6 with $J_{P-F} = 1121$ Hz). Cluster **4** is the first structurally characterized complex containing a μ_4-fluorophosphinidene ligand. Assuming that the fluorophosphinidene ligand is a four-electron donor, the square pyramidal geometry (eight Ru–Ru) is consistent with the 74 valence electron count of the cluster.

Complex **5a** crystallized in the space group $P\bar{1}$ with two independent molecules per unit cell. One of the molecules is disordered, as described below. The molecular structure of the ordered molecule **5a** shown in Fig. 4 consists of tetrahedral dicyclohexyl ammonium cations packed in the crystal lattice with $[Ru_5(CO)_{15}(\mu_4\text{-PO})]^-$ cluster anions. There is a significant hydrogen-bonding interaction between the oxygen atom of the PO ligand and the cation $[H_2NCy_2]^+$ (PO···HN = 1.75 Å). The P–Ru bonds in **5a** are significantly longer [Ru(1)–P = 2.372(2), Ru(2)–P = 2.382(2), Ru(3)–P = 2.369(2), Ru(4)–P = 2.372(2) Å] than those observed for complex **4** and the basal Ru–Ru bond distances for **5a** (Ru–Ru average 2.882 Å) are slightly shorter than those observed in complex **4** (Ru–Ru average 2.919 Å). Thus the substitution of a PO ligand in **5a** for μ_4-PF in **4** has caused a significant change in Ru–P and basal Ru–Ru bond lengths. A simplistic explanation of these facts is that stronger phosphorus bonding to the *exo*-cage atom (oxygen) weakens phosphorus bonding to the Ru_5 core and strengthens metal–metal bonding.

The P–O distance in **5a** (1.512(5) Å) is 0.083 Å shorter than the P–F bond length (1.595(2) Å) in **4** and is at the high end of the range of P=O bond lengths of 1.48–1.52 Å in μ_3-PO clusters [4,6]. This is consistent with the higher coordination number of phosphorus in the μ_4-PO cluster **5a**. There are two other notable aspects of the P–O bond length in **5a** and other complexes containing coordinated PO ligands. First of all, the bond distances are similar to the bond length determined for free PO in molecular beams and matrices (1.476 Å) [1] where the PO molecule has substantial P–O multiple-bond character. Secondly, these P=O bond lengths in PO complexes are substantially shorter than the corresponding P–O bond lengths in clusters containing μ-POR ligands. In this study we can make a direct comparison between the P–O distances in $[H_2NCy_2][Ru_5(CO)_{15}(\mu_4\text{-PO})]$ (**5a**) (P–O = 1.516(4) Å), and the methoxyphosphinidene cluster $Ru_5(CO)_{15}(\mu_4$-POMe) (**6a**) (P–O = 1.609(2) Å). Since both clusters have the same $Ru_5(CO)_{15}$ framework, the conclusion that the PO ligand in **5a** has substantial multiple-bond character as represented by the canonical form $:\dot{P}{=}\ddot{O}$ rather than single-bond character as represented by $:\overset{+}{\dot{P}}{-}\overset{-}{\ddot{O}}:$ seems well justified.

Spectroscopically **5a** is characterized by a medium strong ν(P=O) band in the infrared spectrum at 1064 cm^{-1} and by a ^{31}P resonance at low field ($\delta = 515$ ppm). Complex **5a** is the first example of a cluster complex containing a μ_4-phosphorus monoxide ligand. Counting the anionic phosphorus monoxide ligand as a four-electron donor, then the molecule has 74 valence electrons and eight metal–metal bonds, as required by the effective atomic number rule.

The second independent molecule of **5a** is disordered. The disorder can be described as three molecules with occupancies of 50, 18 and 32% differing in position by a 25 and 28° rotation around the fourfold axis of the μ_4-phosphorus atom. This rotation is accompanied by an approximate 5° tilt off the fourfold axis of the starting complex. The counter ion $[H_2NCy_2]^+$ is also disordered in three positions with occupancies of 50, 15 and 35%.

The molecular structure of the methoxyphosphinidene cluster **6a** is shown in Fig. 5. The core Ru_5P framework is similar to those in **3a**, **4** and **5** with the phosphinidene ligand symmetrically bonded to the square face of the Ru_5 pyramid (Ru(1)–P = 2.3583(8), Ru(2)–P = 2.3329(8), Ru(3)–P = 2.3720(8) and Ru(4)–P = 2.3201(8) Å). The basal Ru–Ru distances average 2.894 Å, slightly shorter than in **4** and very similar to **5a** (average 2.882 Å). Within the methoxyphosphinidene ligand, the PO bond distance is 1.609 (2) Å which is consistent with other complexes containing strong P–O single bonds (compare P–O = 1.613(3) Å in $Ru_4(CO)_{13}(\mu_3$-POMe)). The P–O–C(1) bond angle of 124.7(2) is much larger than the tetrahedral value of 109° and may reflect the presence of some P–O multiple-bond character. Clusters with μ_4-methoxyphosphinidene ligands are rare and previous examples have generally been the serendipitous products of cluster fragmentation or condensation reactions. The route to **6a** is the first rational synthesis of such molecules. The ^{31}P-NMR chemical shift of **6a** is at very low field, namely 542.8 ppm.

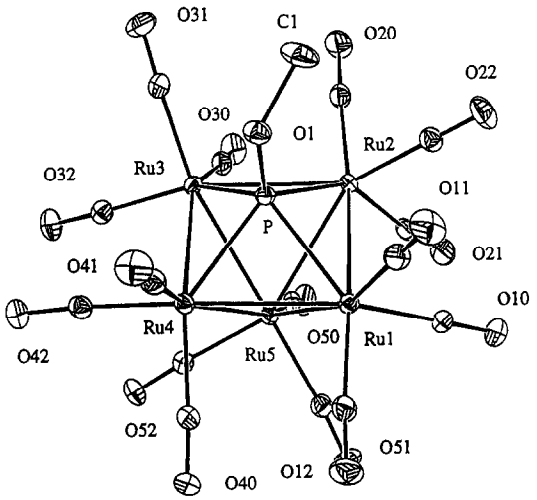

Fig. 5. An ORTEP diagram of $Ru_5(CO)_{15}(\mu_4$-POMe) (**6a**) showing 30% probability thermal ellipsoids. Hydrogen atoms were omitted for clarity. Selected bond lengths (Å) and angles (°): Ru(1)–Ru(2) = 2.8741(3), Ru(1)–Ru(4) = 2.8767(4), Ru(2)–Ru(3) = 2.9002(3), Ru(3)–Ru(4) = 2.9264(3), Ru(5)–Ru(3) = 2.7869(3), Ru(1)–Ru(5) = 2.8431(3), Ru(4)–Ru(5) = 2.8348(3), Ru(5)–Ru(2) = 2.8625(3), Ru(1)–P = 2.3583(8), Ru(2)–P = 2.3329(8), Ru(3)–P = 2.3720(8), Ru(4)–P = 2.3201(8), P–O = 1.609(2), P–O–C(1) = 124.7(2).

Table 2
^{31}P chemical shift data for $Ru_5(CO)_{15}PR$

Compound	Chemical shift versus 80% H_3PO_4
$Ru_5(CO)_{15}(PF)$ [a]	548
$Ru_5(CO)_{15}(POMe)$ [a]	543
$Ru_5(CO)_{15}(POEt)$ [a]	537
$Ru_5(CO)_{15}(PO^iPr)$ [a]	534
$[Ru_5(CO)_{15}(PO)][H_2N(Cy)_2]$ [a]	515
$[Ru_5(CO)_{15}(PO)][H_2N(^iPr)_2]$ [a]	514
$Ru_5(CO)_{15}[PN(Cy)_2]$ [a]	490
$Ru_5(CO)_{15}[PN(^iPr)_2]$ [a]	489
$Ru_5(CO)_{15}(PEt)$ [b]	435
$Ru_5(CO)_{15}(PPh)$ [b]	434
$Ru_5(CO)_{15}(PCH_2Ph)$ [b]	430
$Ru_5(CO)_{15}(PMe)$ [b]	417

[a] In $CDCl_3$.
[b] In toluene-d_8, from Ref. [12].

Upon examination of the ^{31}P chemical shift data (Table 2) for this family of compounds, $Ru_5(CO)_{15}(\mu_4$-PR), it is clear that a trend to lower fields occurs with the introduction of more electronegative R groups. From the data, there appear to be four distinct groups of compounds. The groups with the largest downfield chemical shifts have PF and POR ligands. The next group consists of the P=O complexes. The aminophosphinidene-containing complexes are at higher fields and the compounds that are the least deshielded are the alkyl- and aryl-substituted phosphinidene-containing complexes. These correlations fit in well with previous, more limited $\delta(^{31}P)$ values for such ligands [12,13,22]. The origins of the very large isotropic chemical shifts in such phosphinidene clusters have been analyzed recently by ^{31}P single-crystal and CP MAS NMR spectroscopy [23].

5. Conclusions

In this paper we have described a new methodology for the high-yield synthesis of μ_4-phosphinidene cluster complexes of the type $Ru_5(CO)_{15}(\mu_4$-PNR). This methodology can in turn be used as a general high-yield route to a variety of M_5 μ_4-phosphinidene complexes. We also report, for the first time, the synthesis of clusters containing a μ_4-fluorophosphinidene ligand $Ru_5(CO)_{15}(\mu_4$-PF) (**4**) and a μ_4-phosphorus monoxide ligand, $[R_2NH_2][Ru_5(CO)_{15}(\mu_4$-PO)] (**5**). Structural studies have allowed a comparison of the influence of the substituent on phosphorus [PR = PN^iPr_2, $PNCy_2$, PF, P=O$^-$, POR′ (R = Me, Et, ^{i}Pr)] on bonding of these μ_4-ligands to the Ru_5 cluster framework.

6. Supplementary material

Texts describing full details of the crystal structure analyses for compounds **2a**, **3a**, **4**, **5a** and **6a** including tables of bond distances and angles, atomic coordinates, anisotropic thermal parameters (27 pages). Crystallographic data have been deposited with the Cambridge Crystallographic Database (CCDC nos. 137774–137778) and can be obtained from The Director, CCDC, 12 Union Road, Cambridge CB2 1EZ, UK (fax: +44-1223-336033; e-mail: deposit@ccdc.cam.ac.uk or www:http://www.ccdc.cam.ac.uk) and structure factors are available from the authors on request.

Acknowledgements

This work was supported by grants from the National Research Council of Canada and the Natural Sciences and Engineering Research Council of Canada (to A.J.C.).

References

[1] (a) T.A. Ngo, M. DaPaz, B. Coquart, C. Couet, Can. J. Phys. 52 (1974) 154. (b) S.N. Ghosh, R.D. Verma, J. Mol. Spectrosc. 72 (1978) 200. (c) M. Larzilliere, M.E. Jacox, J. Mol. Spectrosc. 79 (1980) 132. (d) K. Kawaguchi, S. Saito, E. Hirota, J. Chem. Phys. 79 (1983) 629. (e) R.D. Verma, Ch. F. McCarthy, Can. J. Phys. 61 (1983) 1149. (f) K. Kawaguchi, S. Saito, E. Hirota, N. Ohashi, J. Chem. Phys. 82 (1985) 4893. (g) P.A. Hamilton, J. Chem. Phys. 86 (1987) 33. (h) L. Andrews, R. Withnall, J. Am. Chem. Soc. 110 (1988) 5605. (i) R. Withnall, L. Andrews, J. Phys. Chem. 92 (1988) 4610. (j) R. Withnall, M. McCluskey, L. Andrews, J. Phys. Chem. 93 (1989) 126. (k) L. Andrews, M. McCluskey, Z. Mielke, R. Withnall, J. Mol. Struct. 222 (1990) 95. (l) H.E. Matthews, P.A. Feldman, P.F. Bernath, Astrophys. J. 312 (1987) 358.

[2] (a) B.F.G. Johnson, J.A. McCleverty, Prog. Inorg. Chem. 7 (1966) 277. (b) W.P. Griffith, Adv. Organomet. Chem. 7 (1968) 211. (c) N.G. Connelly, Inorg. Chim. Acta Rev. (1972) 47. (d) J.H. Enemark, R.D. Feltham, Coord. Chem. Rev. 13 (1974) 339. (e) R. Eisenberg, C.D. Meyer, Acc. Chem. Res. 8 (1975) 26. (f) F. Bottomley, Acc. Chem. Res. 11 (1978) 158. (g) J.A. McCleverty, Chem. Rev. 79 (1979) 53.

[3] (a) O.J. Scherer, J. Braun, P. Walther, G. Heckmann, G. Wolmershauser, Angew. Chem. Int. Engl. 30 (1991) 852. (b) O.J. Scherer, C. Vondung, G. Wolmershauser, Angew. Chem. Int. Engl. 36 (1997) 1303.

[4] (a) J.F. Corrigan, S. Doherty, N.J. Taylor, A.J. Carty, J. Am. Chem. Soc. 116 (1994) 9799. (b) W. Wang, J.F. Corrigan, S. Doherty, G.D. Enright, N.J. Taylor, A.J. Carty, Organometallics 15 (1996) 2770. (c) W. Wang, A.J. Carty, New J. Chem. 21 (1997) 773. (d) W. Wang, G.D. Enright, J. Driediger, A.J. Carty, J. Organomet. Chem. 541 (1997) 461. (e) W. Wang, G.D. Enright, A.J. Carty, J. Am. Chem. Soc. 119 (1997) 12370.

[5] M.J.A. Johnson, A.L. Odom, C.C. Cummins, Chem. Commun. (Cambridge) (1997) 1523.

[6] (a) J. Foerstner, F. Olbrich, H. Butenschon, Angew. Chem. Int. Ed. Engl. 35 (1996) 1234. (b) J.E. Davies, M.C. Klunduk, M.J. Mays, P.R. Raithby, G.P. Shields, P.K. Tompkin, J. Chem. Soc. Dalton Trans. (1997) 715.

[7] J.H. Yamamoto, K.A. Udachin, G.D. Enright, A.J. Carty, Chem. Commun. (Cambridge) (1998) 2259.

[8] R. Huq, A.J. Poe, S. Chawla, Inorg. Chim. Acta 38 (1980) 121.

[9] E.J. Gabe, Y. Le Page, J.P. Charland, F.L. Lee, P.S. White, J. Appl. Cryst. 22 (1989) 384.

[10] International Tables for X-ray Crystallography, vol. IV, Table 2.2B, Kynoch, Birmingham, 1975, pp. 99–101.

[11] International Tables for X-ray Crystallography, vol. IV, Table 2.3.1, Kynoch, Birmingham, 1975, pp. 149–150.

[12] K. Natarajan, L. Zsolnai, G. Huttner, J. Organomet. Chem. 209 (1981) 85.

[13] (a) A.A. Cherkas, J.F. Corrigan, S. Doherty, S.A. MacLaughlin, F. Van Gastel, N.J. Taylor, A.J. Carty, Inorg. Chem. 32 (1993) 1662. (b) F. Van Gastel, N.J. Taylor, A.J. Carty, Inorg. Chem. 28 (1989) 384. (c) S.A. MacLaughlin, A.J. Carty, N.J. Taylor, Can. J. Chem. 60 (1982) 87.

[14] J.M. Fernandez, B.F.G. Johnson, J. Lewis, P.R. Raithby, J. Chem. Soc. Chem Commun. (1978) 1015.

[15] D.W.J. Cruickshank, Acta Crystallogr. 17 (1964) 671.

[16] M.J.E. Hewlins, J. Chem. Soc. B (1971) 942.

[17] L. Pauling, The Nature of the Chemical Bond, third ed., Cornell University, Ithaca, New York, 1960.

[18] (a) F. Iwaski, M.J. Mays, P.R. Raithby, P.L. Taylor, P. Wheatley, J. Organomet. Chem. 213 (1981) 185. (b) A.J. Carty, Pure Appl. Chem. 54 (1982) 113. (c) J. Schneider, L. Zsolnai, G. Huttner, Chem. Ber. 115 (1982) 989.

[19] W. Wang, J.F. Corrigan, G.D. Enright, N.J. Taylor, A.J. Carty, Organometallics 17 (1998) 427.

[20] S. Kahlal, K.A. Udachin, L. Scoles, A.J. Carty, J.-Y. Saillard (2000) submitted.

[21] F.H. Allen, O. Kennard, D.G. Watson, L. Brammer, A.G. Orpen, R. Taylor, J. Chem. Soc. Perkin. Trans. II (1987) S1.

[22] S.A. MacLaughlin, D. Nucciarone, A.J. Carty, in: J.G. Verkade, L.D. Quinn (Eds.), Phosphorus 31-NMR Spectroscopy in Stereochemical Analysis: Organic Compounds and Metal Complexes, vol. 11, VCH, New York, 1986, p. 559 Ch. 11.

[23] K. Eichele, R.E. Wasylishen, J.F. Corrigan, N.J. Taylor, A.J. Carty, J. Am. Chem. Soc. 117 (1995) 6961.